XI International Conference on Computational Plasticity. Fundamentals and Applications
COMPLAS XI
E. Oñate, D.R.J. Owen, D. Peric and B. Suárez (Eds)

Dynamic Localizations in Structural Steel at High Strain Rates and Temperatures – COMPLAS XI

FARID H. ABED[*] AND FADI S. MAKAREM[*]

[*]Department of Civil Engineering
American University of Sharjah
Sharjah, P.O.Box 26666, United Arab Emirates
E-mail: fabed@aus.edu, web page: http://www.aus.edu

Key words: HSLA-65, DH-36, Flow stress, Shear band, Hat-shaped specimen.

Abstract. The proposed paper presents a numerical study on the formation of shear bands at localized regions in two ferrite steel alloys, HSLA-65 and DH-36, subjected to certain range of velocity impact. Constitutive relations developed by the author [1] for ferritic steels is utilized in simulating the thermal and athermal parts of the flow stress over a wide range of temperatures and strain rates. The proposed plasticity model is implemented into the commercially well-known finite element software ABAQUS through VUMAT user subroutine. This implementation enables studying the shear band formation over a wide range of initial temperatures and strain rates in a cylindrical hat-shaped specimen with certain dimensions where the location of shear localization preceding shear band formation is forced to be between the hat and the brim. Sensitivity analysis is performed on different mesh configurations in order to select the optimum mesh. Another sensitivity analysis is also performed on the constitutive plasticity model material parameters to study their effect on the shear bands formation. Several conclusions related to the width of the shear bands considering the velocity load and initial temperatures will be discussed throughout this work.

1 INTRODUCTION

Numerous studies on the formation of shear bands (shear localization) were conducted due to their importance as deformation mechanism especially during high speed loading (i.e. impact loading). The high concentration of strains in a particular location of a steel structure is a physical phenomenon that can be observed in reality and in laboratory testing. Areas of high strain concentrations can be developed in specimens prepared in the lab and tested under wide range of strain rates and temperatures. Even when the strain rate is low, the increase of plastic strains in the areas of strain concentration is fast and associated with higher than average dissipation of energy. Studying the development of shear bands is very important because they dominate the deformation and fracture modes in many metals. It is usual to observe strain localization in ductile materials like metals, but also can be observed in composite structures made of brittle and ductile components. The newly developed physically based constitutive viscoplastic model by the author [1] is utilized in investigating shear localization in ferrite steel over wide range of temperatures and strain rates. This proposed model is implemented in the well-known commercial finite element software ABAQUS

through the material subroutine VUMAT. This implementation is utilized in this study to investigate the dynamic simulation of adiabatic shear localization in a cylindrical hat-shaped sample where large shear strains are generated in a small region during compression mode [2].

Two high strength steels were considered in the proposed comparisons: DH-36 and HSLA-65 that are used in naval and other structural applications. They may be subjected, in their naval use, to high-rate loading due to collision or impact which, in turn, requires high toughness and high strength under variable conditions including various temperatures and strain rates. High strength low alloy (HSLA) steels were first used in 1960s by developing alloy of low-carbon steels with Niobium (Nb), Vanadium (V) and Titanium (Ti). HSLA-65 was recently developed with 65 ksi (450MPa) yield strength allowing the use of thinner plates to reduce the weight of the structure. DH-36 is commonly used in the manufacture of vessels and submarines. As ship hull steel, especially in high-speed sealift vessels, it may be subjected to high-rate loading due to collision, impact, or explosion. The major alloy content of the two investigated steels is given by Nemat-Nasser and Guo [3-4]. In addition to more than 97% of iron, the microstructure of HSLA-65 and DH-36 is mainly composed, of 1.4% and 1.37% of Manganese (Mn), 0.24% and 0.22% of Silicon (Si), and 0.08% and 0.14% of Carbon (C), respectively. Moreover, the alloy content of HSLA-65 contains very small portion of copper (<0.01%) as compared to DH-36 (0.14%).

2 MICROSTRUCTURE-BASED VISCOPLASTICITY IN FERRITIC STEEL

Accurate determination of plasticity models capable of predicting the flow stress of metals in general and steel in particular is not easy because of the coupling effects of strain, strain rate and temperature. The flow stress dependency of the above-mentioned three parameters becomes very significant at higher temperatures and strain rates. It was observed experimentally by different authors that the variation of stress strain curves at a certain strain rate and different temperatures or at certain temperature and different strain rates appear at yielding point and almost no variation was noticed in the hardening curves. The proposed model additively decomposes the flow stress into athermal and thermal components which coincides with the experimental observation. The athermal component is independent of strain rate and related to strain hardening, *R(p)*, and small portion of the yield stress, Y_a. The thermal component is mainly controlled by yield stress and shows a coupled effect of temperature and strain rate. The static definition of the yield function represented by the athermal flow stress is shown in Eq. (1):

$$f = \sigma_{eq} - Y_a - R(p) \tag{1}$$

The thermal component represents the dynamic stress that exceeds the static yield surface. This stress is related to the reference viscosity, η_o^{vp}, and threshold yield stress, $\hat{Y}$. The reference viscosity is the minimum value that can be achieved at very high temperature. The viscosity parameter (known as relaxation time), η^{vp}, is very important when it comes to finite element implementation of viscoplasticity because it helps in introducing a physical length

scale that is used in regularizing some problems encountered in finite elements computation. It also allows the spatial difference operator in the governing equations to retain its ellipticity. The dynamic stress is presented by Eq. (2) and viscoplastic multiplier is shown in Eq. (3) by rearranging Eq. (2).

$$\sigma_{th}^{v} = \hat{Y}(1-(-\beta_2 T \ln(\eta_o^{vp}\dot{\lambda}^{vp}))^{\frac{1}{q_1}})^{\frac{1}{q_2}} \tag{2}$$

$$\dot{\lambda}^{vp} = \frac{1}{\eta^{vp}(T)}\varphi(\sigma_{th}^{v}, T, \hat{Y}) \tag{3}$$

The overstress function presented in Eq. (4) and the viscosity parameter shown in Eq. (5) are explicitly temperature related variables. $\hat{Y}$ is chosen in normalizing the overstress function.

$$\varphi(\sigma_{th}^{v}, T, \hat{Y}) = \exp\left(1 - \frac{\left(1-\left(\frac{\sigma_{th}^{v}}{\hat{Y}}\right)^{q_2}\right)^{q_1}}{\beta_2 T}\right) \tag{4}$$

$$\eta^{vp} = \eta_o^{vp}\exp\left(\frac{1}{\beta_2 T}\right) \tag{5}$$

The hardening *R(p)* which is strain dependent component of flow stress is defined in Eq. (6).

$$R(p) = \bar{B}(1-e^{-kp})^{\frac{1}{2}} \tag{6}$$

where the reference viscosity parameter, the threshold yield stress, the athermal yield stress and the parameter β_2, $\bar{B}$ are related to the microstructure physical quantities as follows:

$$\bar{B} = m\alpha\mu b\left(\frac{m}{k}\right)^{\frac{1}{2}};\ \ \eta_o^{vp} = (\bar{m}\, b\rho_i d)^{-1} t_{wo}$$

$$\hat{Y} = m\alpha_0\mu_o\frac{b^2}{A_0};\ Y_a = \alpha\mu\left(\frac{b}{D_g}\right)^{\frac{1}{2}};\ \ \beta_2 = \frac{K}{G_o} \tag{7}$$

Where *b* is the magnitude of the Burger vector, *m* is the orientation factor that relates the shear stress to the normal stress $\sigma = m\tau$ where $m = \sqrt{3}$ for the case of the von Mises flow rule, μ is the shear modulus; α is an empirical coefficient, *K* is the Boltzmann's constant, G_o is the Gibbs energy at zero Kelvin temperature, *M* represents the dislocation multiplication factor, *k* is the annihilation factor, D_g is the grain size, t_w is the time that a dislocation wait at

an obstacle and t_{wo} is the lowest value, $\bar{m} = \sqrt{M_{ij}M_{ij}}$ where M_{ij} is the Schmidt orientation tensor, d is average distance the dislocation moves between the obstacles, $\rho_i = l_i^{-2}$ is the initial dislocation density and l_i is the initial dislocation distance. An explicit definition of the length scale parameter l which is taken as initial value of dislocation distance can be derived in terms of microstructure physical quantities by rearranging the definition of the viscosity parameter in Eq. (7) as follows:

$$l = \left(ac\eta_o^{vp}\right)^{\frac{1}{2}}, \quad \text{where: } a = \bar{m}b\,; \quad c = d/t_w \tag{8}$$

The c parameter in Eq. (8) is actually the elastic wave propagation velocity in the material whereas a parameter is a proportional factor that depends on the particular initial boundary value problem under consideration. Once the viscosity parameter is calculated, the viscoplastic strain tensor is obtained by the following relation:

$$\hat{d}^{vp} = \dot{\lambda}^{vp} N = \dot{\lambda}^{vp} \frac{\partial f}{\partial \tau} = \dot{\lambda}^{vp} \frac{\partial \sigma^{eq}}{\partial \tau} \tag{9}$$

Where: $\partial\sigma^{eq} = (3\tau_{ij}\tau_{ij}/2)^{1/2}$ represents the equivalent stress, which is defined based on von Mises yield criterion in terms of the deviatoric stress, $\tau_{ij} = \sigma_{ij} - \sigma_{mm}\delta_{ij}/3$. The evolution equation for the dislocation density utilized in deriving the proposed ferrite steel model resulted in an exponential relation for the strain hardening as shown in Eq.(10) which shows the combined athermal and thermal stresses.

$$\sigma = c_1 + c_2\sqrt{1 - e^{-c_3\varepsilon_p}} + c_4(1 - (c_5T - c_6T\ln\dot{\varepsilon}_p)^{1/q_1})^{1/q_2} \tag{10}$$

The material parameters c_1–c_6 appeared in the above constitutive relations are related to the microstructure physical quantities as explained before in Eq. (7) as follows:

$$c_1 = Y_a\,;\ c_2 = \bar{B}\,;\ c_3 = k\,;\ c_4 = \hat{Y}\,;\ c_5 = \beta_2 \ln\left(\frac{1}{\eta_o^{vp}}\right);\ c_6 = \beta_2 \tag{11}$$

The above relation clearly shows the coupling effect of strain rate and temperature on the yield stress where σ is the equivalent stress, ε_p is the equivalent plastic strain, $\dot{\varepsilon}_p$ is the equivalent plastic strain rate, T is the temperature in Kelvin, and q_1 & q_2 are constants defining the shape of the short-range barriers. The material constants c_2 *and* c_3 define the strain dependent athermal component of the flow stress, c_1 represents an additional athermal stress, c_4 represents the threshold yield stress at which the dislocation can overcome the barriers without the assistance of thermal activation, c_5 and c_6 are two thermal activation parameters characterizing the thermal component of the flow stress and are related to the reference Gibbs energy at zero absolute temperature, Boltzmann's constant, reference dislocation velocity, and initial dislocation density [1]. In Eq. (10), the thermal component of

the flow stress is non-negative, thus, the term $(c_5 T - c_6 T \ln \dot{\varepsilon}_p)$ should be set equal to zero when the temperature exceeds the critical value. The critical temperature defines the stage of deformation at which the thermal stress is completely vanished. This critical value; however, is strain rate dependent and can be defined as follows:

$$T_{cr} = (c_5 - c_6 \ln \dot{\varepsilon}_p)^{-1} \tag{12}$$

3 SHEAR LOCALIZATION IN CLYNDYRICAL HAT-SHAPED SAMPLES

The developed constitutive model is implemented in ABAQUS via user's material subroutine VUMAT. ABAQUS/Explicit version is used to perform finite element simulation on hat-shaped modeled specimens and to investigate the formation of shear bands in ferrite steel such as HSLA-65 and DH-36. Experimental investigation of the dynamic deformation response of hat-shaped specimen shown schematically in Figure 1(a) was adopted by different authors. The dimensions of the specimens used in these studies differ from one author to another. The dimensions of the hat-shaped sample used in this study are presented in Table 1 and correspond to a study done by Perez-Prado [6]. The geometry was chosen in such a way that the inner diameter of the brim is shorter than the inner diameter of the hat by approximately 4.5% in order to sustain large amount of shear strain.

Table 1: Dimensions (mm) for ferrite steel hat-shaped sample

r_1	r_2	r_3	h_1	h_2	h_3
9.53	4.85	5.08	15	7.0	6.97

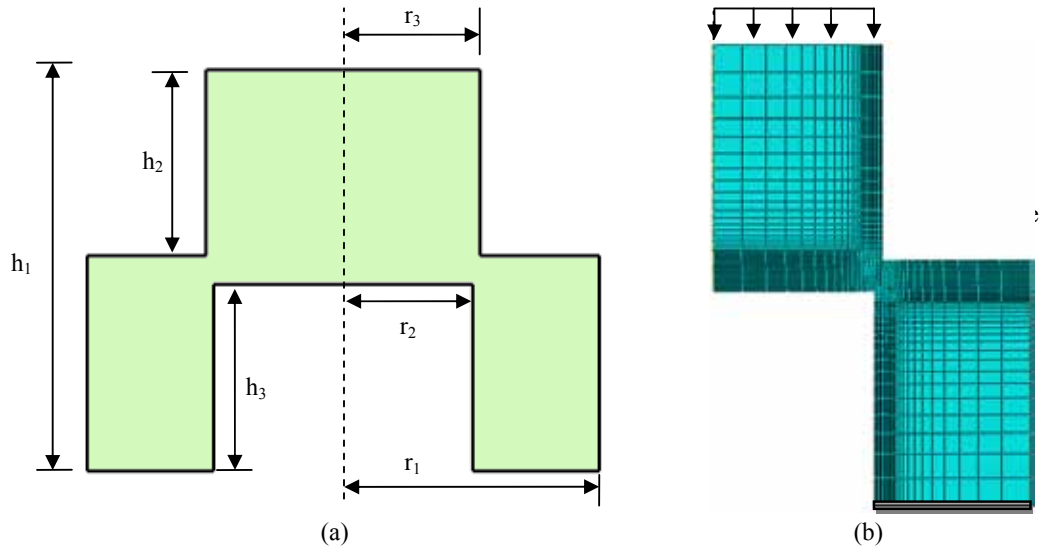

Figure 1: (a) geometric description of the cylindrical hat-shaped specimen (b) FE model for a quarter portion of the hat-shaped specimen using axisymmetric mesh elements.

The geometry of the hat-shaped specimen enables modeling it using four-node axisymmetric elements of CAX4R ABAQUS type with shear region zone limited between the upper hat and lower brim portions. The advantage of the hat-shaped specimen is that the location of shear localization preceding shear band formation is forced to be between the hat and the brim. This is because the dimensions of the specimen were chosen in this study so that there is mismatching between inner radius of the brim (r_2) and the hat radius (r_3) to create an overlapping region. A region of high strain concentration is created as a consequence. The axisymmetric specimen is subjected to compression dynamic velocity load from the top at the hat and movement is restrained at the bottom as illustrated in Figure 1(b).

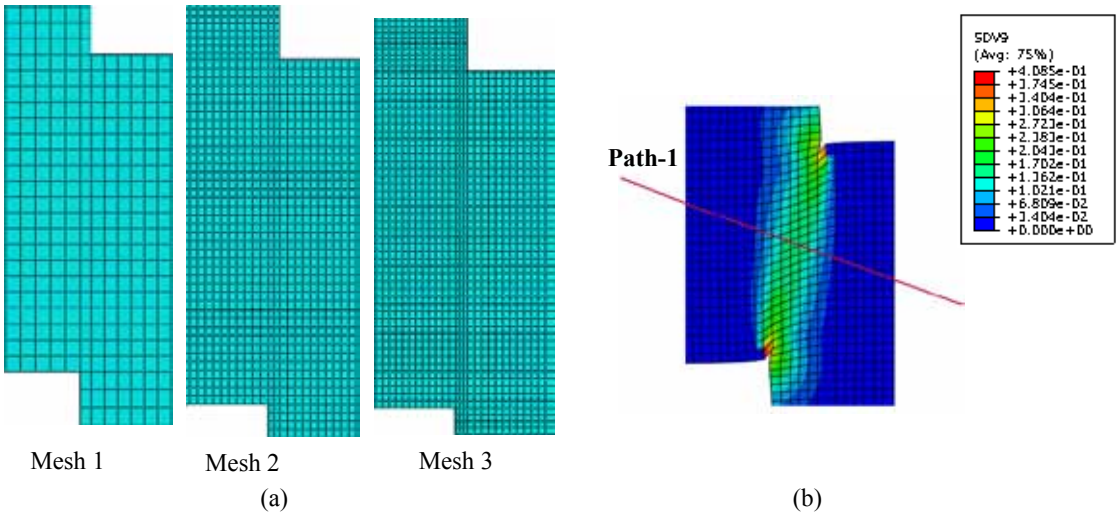

Figure 2: (a) Mesh refinements in the shear zone (b) Path 1 through the shear zone of the hat-shaped specimen

Three different mesh configurations were used to mesh the model geometry and the region of shear deformation as shown in Figure 2 (a). Mesh 1 represents a coarse mesh whereas Meshes 2 and 3 are of higher resolution. Figure 2(b) shows true path distance (Path-1) passing through the shear zone and perpendicular to the shear band. Simulations were carried out with the three mesh configurations to study the sensitivity of the results to mesh refinement. It was found out that shear stress-displacement curve presented in Figure 3(a) and plotted for an element located in the middle of the shear zone is not varying much when comparing with meshes 2 and 3. The same observation regarding mesh sensitivity was noticed when plotting the equivalent plastic strain along path1 as presented in Figure 3(b). It is obvious that the coarse mesh 1 is not able to capture a reasonable value for the equivalent plastic strain along the same true path and is of no match to the results obtained from meshes 2 and 3. Mesh 2 was chosen to carry out the rest of the dynamic simulations since it achieved balance between the accuracy of the results and reducing the computational time especially when it comes to dynamic explicit integration computational scheme.

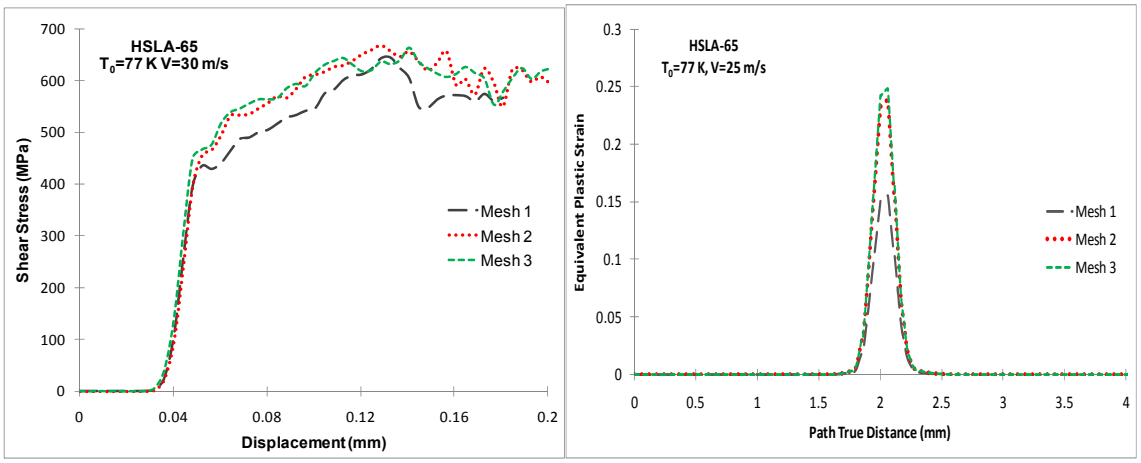

(a) (b)

Figure 3: (a) Shear stress for three different meshes configuration; (b) Distribution of the equivalent plastic strain for HSLA-65 across path 1for different meshes configuration.

4 NUMERICAL SIMULATIONS RESULTS

The axisymmetric model was subjected to wide range of velocities and initial temperatures. The velocities applied were 0.5 m/s, 1 m/s 10 m/s, 20 m/s and 30 m/s whereas the temperatures were 77 K, 200 K, 296 K, 400 K and 500 K. The modeled specimen was dynamically compressed up to a total displacement of 0.20 mm. It was observed that the shear stress first reaches a peak value before it decreases with increasing displacement which means that the hardening mechanism of ferrite steel prevails at the initial stage during plastic deformation. When the plastic deformation evolves, the softening mechanism becomes dominant as heat is accumulating in the shear zone especially when the specimen is subjected to high rate adiabatic deformation. Figure 4 shows contour plot of the equivalent plastic strain (shear bands) in three-dimensional shape corresponding to three fourths of the hat-shaped specimen. The plastic strain concentration is obvious in the shear zone region.

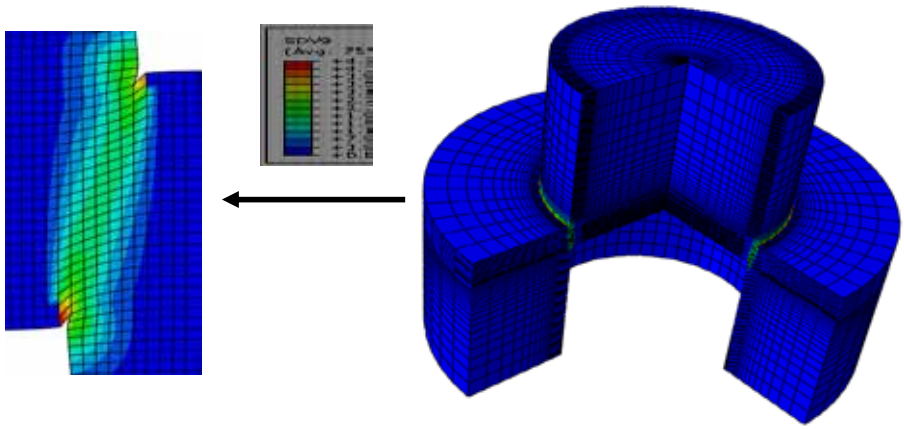

Figure 4: Contour plot of the equivalent plastic strain (shear bands) at velocity =25m/s and T_o = 296 K

A comparison between shear bands corresponding to simulation at different temperatures at the same velocity load is presented in Figures 5 and 6 for both HSLA-65 and DH-36 steels. It was observed that widths of the shear bands increase with temperature increasing. Figure 7 presents the distribution of the equivalent plastic strain in both steels at the end of the applied displacement along Path-1 passing through the center of the shear zone (shear band) at 25 m/s velocity and different temperatures. The distribution of the equivalent plastic strain is interpreted as the shear band width. The figures show that that the plastic strain peak is greatest when the temperature is lowest. For instance, the largest plastic strain is achieved at lowest temperature = 77 K. They also show the shear band width variation with respect to each initial temperature at the same compression velocity load. The widths of the shear zones range approximately from 0.5 to 1.0 mm in both steels depending on the initial temperatures and applied velocities. It can be concluded that the width of the shear band (localization) varies considerably with different initial temperatures.

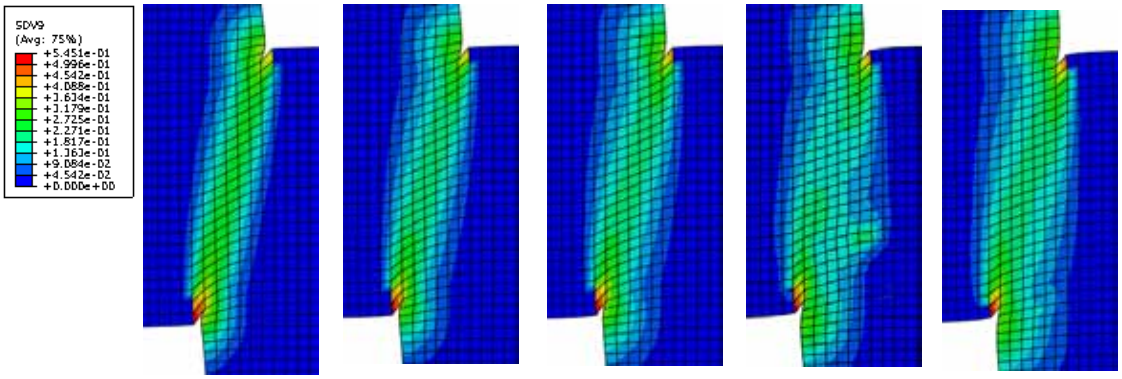

Figure 5: Contours of the equivalent plastic strain (shear bands) at 0.2 mm axial displacement and different temperatures, HSLA-65 Steel at V = 25m/s

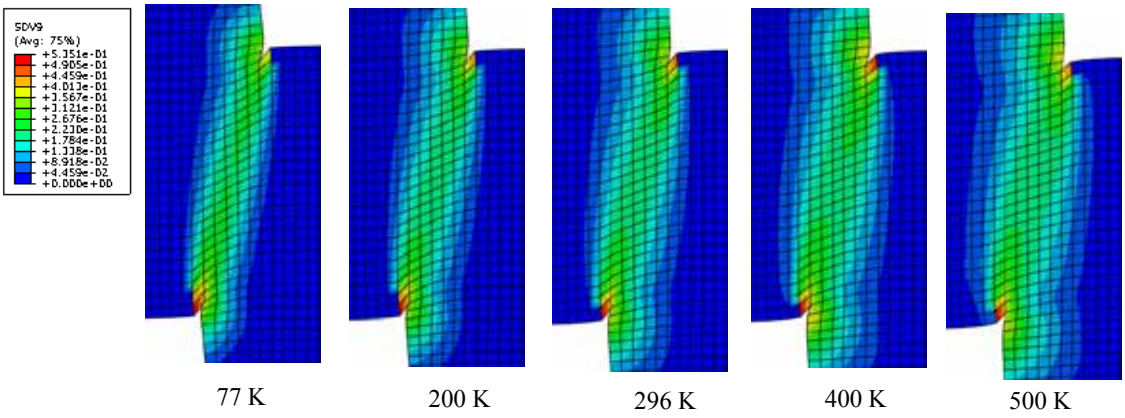

Figure 6: Contours of the equivalent plastic strain (shear bands) at 0.2 mm axial displacement and different temperatures, DH-36 steel at V = 25m/s

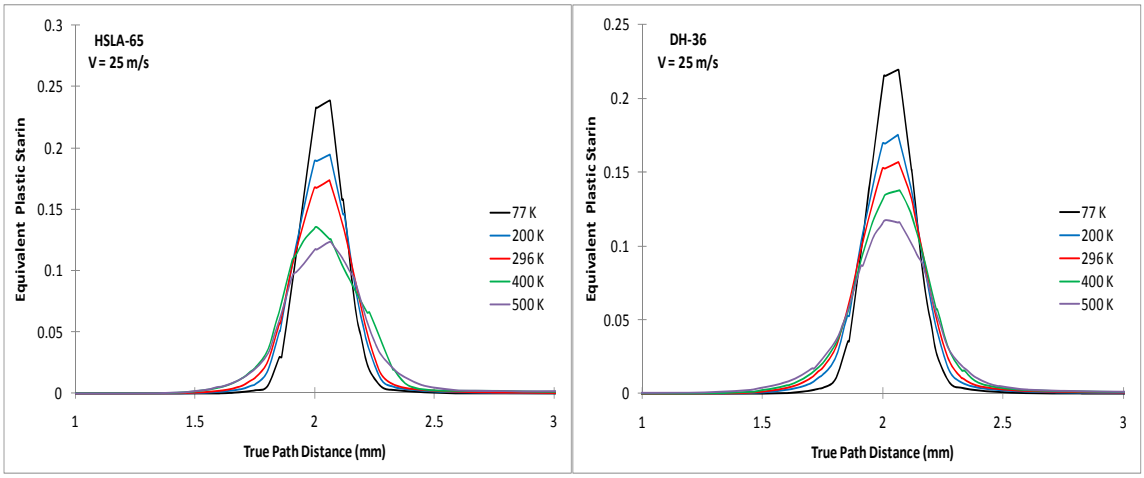

(a) (b)

Figure 7: Equivalent plastic strain at V=25 m/s, 0.2 mm axial displacement and different temperatures along path-1: (a) HSLA-65, (b) DH-36

On the other hand, less variation in the shear bands widths was noticed at different velocities at the same initial temperature as illustrated in Figure 8 which show the equivalent plastic strain distribution along Path-1 at initial temperature of T_o=77 K and different velocities for both steels.

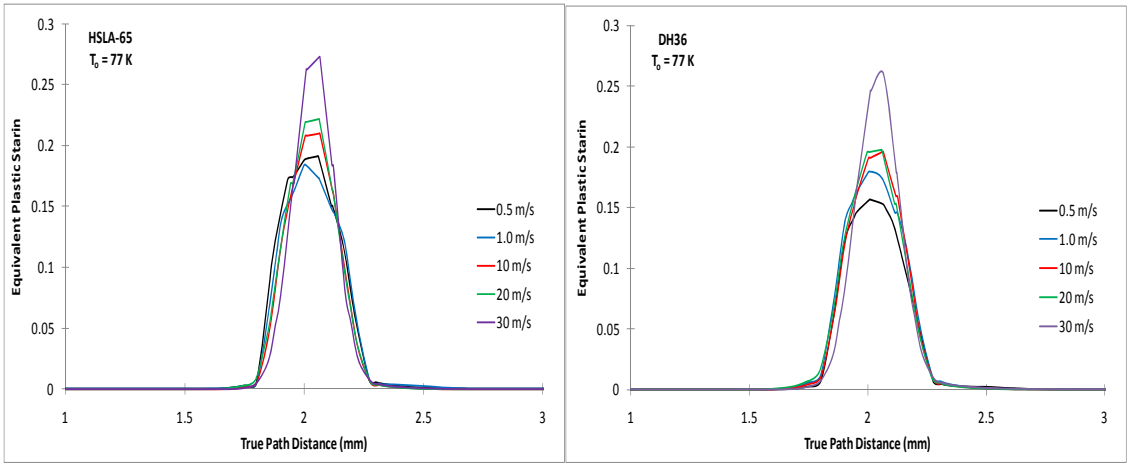

(a) (b)

Figure 8: Equivalent plastic strain at initial T=77K, 0.2mm axial displacement and different velocities: (a) HSLA-65, (b) DH-36

4 MODEL PARAMETERS SENSETIVITY ANALYSIS

Simulating the effect of impact load on steel structures requires choosing a robust plasticity finite element constitutive model. Some of these models are empirically, semi-physical or physically based. In other words, the material parameters of some models are obtained empirically whereas the material parameters in some other models are related to the micro-structure quantities of the material such as the proposed model. Complex statistics methods could be applied on a set of experimental data to determine the material parameters of plasticity model. Certain inaccuracy in the value of the determined material parameter might be encountered during the process of obtaining them which also depends on the accuracy and amount of the experimental data. Hence, it is recommended to study the sensitivity of a certain output to a change in one or more of the material constants. In this study, sensitivity analysis on the six constants of the developed model is performed, c_1,c_2, c_3, c_4, c_5 and c_6. It is expected to detect a change in the shear band width at certain velocity and temperature when changing one of the model parameters while keeping all others constant.

Comparisons between formed shear bands corresponding to simulations at the same conditions (velocity = 10 m/s and temperature = 77K) are conducted for all constants. For better quantification for the shear band width sensitivity to changes in the material parameters, the equivalent plastic strains were plotted along Path-1 which is perpendicular to the shear band. Figure 9 shows a sample of these comparisons for the effect of constant c_5 on the the width of the localized region at the shear zone at 10m/s velocity and 77K initial temperature for both HSLA-65 and DH-36 steels. It is clearly shown that increasing the material constants c_5 which is related to the thermal stress component of the VA model leads to increasing the value of the equivalent plastic strain. The width of the shear zone is increased consequently.

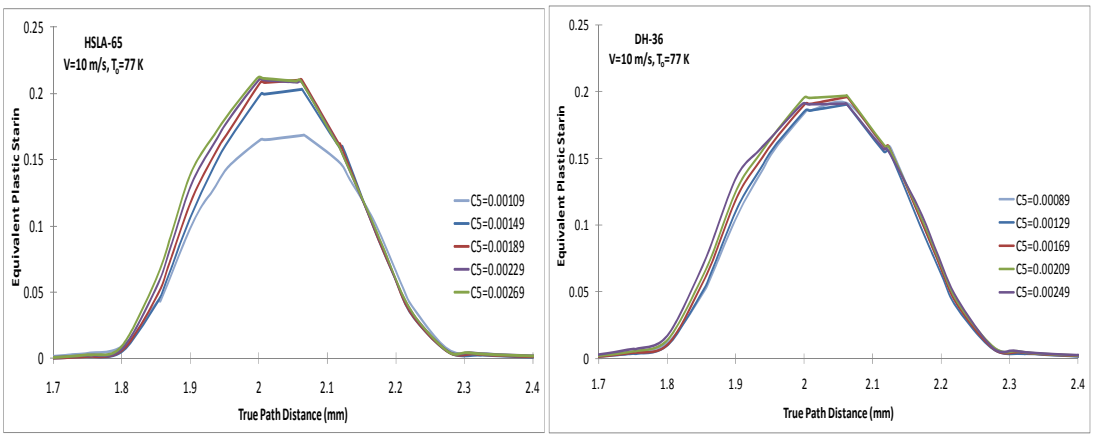

(a) (b)

Figure 9: Equivalent plastic strain when changing the model parameters c_5, at 0.2mm axial displacement for (a) HSLA-65 steel and (b) DH-36 steel.

CONCLUSIONS

In this work, the shear band formation in hat-shaped specimen were studied under different dynamic velocities (0.5, 1.0, 10, 20, 30 m/s) and initial temperatures (77, 200, 296, 400, 500K). The simulations were carried out using the new developed constitute model for ferrite steel after being implemented in ABAQUS via VUMAT user subroutine. It was observed that the width of the shear band increases with increasing the initial temperature in both HSLA-65 and DH-36 steels. The width of the shear band doesn't vary considerably when comparing at several applied dynamic velocities and at the same initial temperature. Sensitivity analysis was also performed on the model constants, by studying their variation effect on the width of the shear band. It was observed that increasing the value of material parameter c_5 increases the width of the shear band.

REFERENCES

[1] Abed, F.H. Constitutive modeling of the mechanical behavior of high strength ferritic steels for static and dynamic applications, *Mech Time-Depend Mater* (2010) **14**: 329-345.

[2] Abed, F.H. and Voyiadjis, G.Z. Adiabatic shear band localizations in BCC metals at high strain rates and various initial temperatures. *International Journal of Multiscale Computational Engineering* (2007) **5:** 325-349.

[3] Nemat Nasser, S. and Guo, W.G. Thermomechanical response of DH-36 structural steel over a wide range of strain rates and temperatures. *Mech Mater* (2003) **35**: 1023-1047.

[4] Nemat Nasser, S. and Guo, W.G. Thermomechanical response of HSLA-65 steel plates: experiments and modeling. *Mech Mater* (2005) **37**: 379-4057.

[5] Voyiadjis, G., and Abed, F., Microstructural Based Models for BCC and FCC Metal with Temperature and Strain Rate Dependency, *Mech Mater* (2005) **37**: 355-378.

[6] Perez-Prado, M.T., Hines, J.A., and Vecchio, K.S. Microstructural evolution in adiabatic shear bands in Ta and Ta-W alloys. *Acta Materialia* (2001) **49**: 2905-2917.